كلية الهندسة بشبرا
FACULTY OF ENGINEERING AT SHOUBRA
ERJ
PRINT ISSN 3009-6049
ONLINE ISSN 3009-6022

ENGINEERING RESEARCH JOURNAL (ERJ)
Volume (53),Issue (2)
April 2024, pp:212-219
https://erjsh.journals.ekb.eg

Groundwater Modeling for Seawater Intrusion Simulation in Coastal Aquifers in Ain Sukhna, Egypt

Alaa Nabil EL-HAZEK [1], Neveen B. Abdelmageed [1], Ahmed El Belasy [2] , Dalia H. Amin [2,*]

[1] *Civil Engineering Department, Faculty of Engineering at Shoubra, Cairo, Benha University, Egypt*
[2] *Water Resources Research Institute, National Water Research Center, Egypt*
**Corresponding author*

E-mail address : alaa_elhazek@yahoo.com , neveenbadawy1975@gmail.com , belasywrri@gmail.com, engdalia.work@gmail.com

Abstract: Seawater intrusion is a vital issue that threatens many coastal aquifers around the world, especially under the current conditions of climate change. One of the susceptible regions is the Ain Sukhna area in Egypt, where there are three promising aquifers that are mainly relied upon for development. This study investigates the initial condition of seawater intrusion impacts in the study area using a 3-D groundwater numerical model that was created and run by MODFLOW and SEAWAT. The model was calibrated and validated for both groundwater head and salinity observed values in 2013 in the steady state and dynamic state. The results showed a good agreement between the calculated and observed values. The results also clarified that both the medium and deep aquifers were affected by the migration of seawater inland more than the shallow aquifer except for the zone having the shale layer that obstructed seawater intrusion slightly.

Keywords: Seawater Intrusion, Ain Sukhna, Numerical Modeling, SEWAT, Visual MODFLOW.

1. Introduction

Seawater intrusion is considered one of the most recent issues affecting the quality of groundwater in coastal areas, especially arid and semi-arid areas, where groundwater is mainly relied upon for development. Ain Sukhna is one of the areas exposed to seawater intrusion, as it contains three coastal aquifers located on the Gulf of Suez. Due to the successive changes in land uses in the region, an increase in groundwater abstraction rates was needed especially with the development of the Suez Canal Economic Zone and the climate change which led to seawater intrusion.

Many studies were conducted about seawater intrusion in Egypt especially for the Nile Delta Aquifer. Abd-Elaty, I. et al., [1], developed an analytical solution for saltwater intrusion in coastal aquifers considering climate change and different boundary conditions. The aim was to develop a new formula to predict the difference in depth of freshwater to seawater interface. This numerical solution was applied at the Middle Nile Delta Aquifer and compared to a numerical solution under different scenarios. The results showed a good agreement between both solutions which confirmed the qualification of using the analytical model for other similar studies. Armanuos, A. M. et al., [2], detected the effects of seawater intrusion for three proposed scenarios including sea level rise, varied groundwater abstraction rates, and a combination of both. The worst-case scenario was the third one that was accompanied by the most increase in seawater intrusion. El Shinawi, A. et al., [3], presented a perspective of seawater intrusion in the Nile Delta Aquifer employing a combination of laboratory and numerical modeling. It was found that sea level rise was an upward force that raised the water table and minimized land subsidence while it was increased due to the effect of over-pumping.

Similarly, many studies were conducted on seawater intrusion worldwide by many authors using numerical modeling such as Yang et al., [4], Janardhana and Khairy, [5], Ranjbar et al., [6], and Mastrocicco et al., [7] or using laboratory experiments such as Brkić and Srzić, [8] or combination of them such as Na et al., [9].

2. MATERIALS AND METHODS

The applied numerical method is the finite difference method using the SEAWAT numeric engine as a simulation tool to model the processes of groundwater flow and transport. SEAWAT combines the flow code (MODFLOW) with the solute-transport code (MT3DMS) in a single code to solve the coupled flow and solute-transport equations, Guo and Langevin, [10].

The governing equations of SEAWAT are derived based on the concept of equivalent freshwater head that is estimated as the freshwater head that replacing the same weight of saline water and could be calculated using the following Equation (1), Guo and Langevin, [10]:

$$h_f = \frac{\rho}{\rho_f} h - \frac{\rho - \rho_f}{\rho_f} z \qquad (1)$$

Where:

h_f is the equivalent freshwater head,

ρ is the density of the native aquifer water [ML^{-3}],

ρ_f is the density of freshwater [ML^{-3}],

and Z is the elevation at the measurement point [L].

Also, for variable-density groundwater flow in terms of the equivalent freshwater head, the governing Equation (2), Guo and Langevin, [10], is:

$$\frac{\partial}{\partial \alpha}\left[\rho K_{f\alpha}\left(\frac{\partial h_f}{\partial \alpha}+\frac{\rho-\rho_f}{\rho_f}\frac{\partial Z}{\partial \alpha}\right)\right]+\frac{\partial}{\partial \beta}\left[\rho K_{f\beta}\left(\frac{\partial h_f}{\partial \beta}+\frac{\rho-\rho_f}{\rho_f}\frac{\partial Z}{\partial \beta}\right)\right]+\frac{\partial}{\partial \gamma}\left[\rho K_{f\gamma}\left(\frac{\partial h_f}{\partial \gamma}+\frac{\rho-\rho_f}{\rho_f}\frac{\partial Z}{\partial \gamma}\right)\right]=\rho S_f\frac{\partial h_f}{\partial t}+\theta\frac{\partial \rho}{\partial C}\frac{\partial C}{\partial t}-\rho_s q_s \qquad (2)$$

Where:

α, β, γ are orthogonal coordinate axes, aligned with the principal directions of permeability,

K_f is equivalent to freshwater hydraulic conductivity [LT^{-1}],

h_f is the equivalent freshwater head,

ρ is the density of the native aquifer water [ML^{-3}],

ρ_s is the fluid density source or sink water [ML^{-3}],

S_f is equivalent freshwater specific storage [L^{-1}],

t is time [T],

θ is effective porosity [dimensionless],

C is solute concentration [ML^{-3}],

and q_s is the volumetric flow rate of sources (positive) and sinks (negative) per unit volume of aquifer [L^3T^{-1}].

The solute transport of contaminants such as salinity in groundwater flow is represented by the following partial differential Equation (3), Zheng and Wang, [11]:

$$\frac{\partial(\theta C^k)}{\partial t}=\frac{\partial}{\partial x_i}\left(\theta D_{ij}\frac{\partial C^k}{\partial x_j}\right)-\frac{\partial}{\partial x}(\theta v_i C^k)+q_s C_k^s+\sum R_n \qquad (3)$$

Where:

θ is the porosity of the subsurface medium,

C^K is the dissolved concentration of species k [ML^{-3}],

D_{ij} is the hydrodynamic dispersion tensor [L^2T^{-1}],

v_i is seepage or linear pore water velocity [LT^{-1}],

q_s is the volumetric flow rate per unit volume of aquifer representing fluid sources and sinks [L^3T^{-1}],

C_k^s is the concentration of the source or sink flux for species k [ML^{-3}],

And $\sum R_n$ is the chemical reaction term [$ML^{-3}T^{-1}$].

Developing a model for the groundwater system in the study area requires the following:

a. Defining the hydraulic boundaries of the study area.

b. Knowing the hydraulic properties of the aquifers including the hydraulic conductivity, transmissivity, and storage coefficient values.

c. Detecting the aquifer main recharge resulting from the two sources in the study area (rainfall and floods of wadis).

d. Gathering data of wells including groundwater level measurements, groundwater salinity measurements, discharging rates of the wells and design of wells, and borehole logs from reports of drilling wells.

3. STUDY AREA

The study area lies in the northwestern part of the Gulf of Suez and covers an area of about 400 km^2. It is enclosed between latitudes 29° 31' 03" and 29° 46' 04" N and longitudes 31° 58' 58" and 32° 24' 51" E. Mountain ranges are bounding the study area westward which extending from Mount Ataka at the far north of the Gulf of Suez to Mount El-Galala El-Bahariya in the south. As shown in Figure (1), four wadis exist on the western side between mountains, which are Wadi Hommath, Wadi Hagoul, Wadi Bada, and Wadi Ghweiba.

FIGURE (1). A Map of the Wadis of Study Area, EL-HAZEK et al., [12].

The study area consists of three main geomorphological units including flat areas at the main streams of the wadis and its tributaries as well as the delta of wadis and terraces as discrete zones at the middle and northern parts of the study area. Mountainous areas extend to northern western, north, and southern parts of the study area. The geologic characteristics of the study area involve different lithological units with different ages varying from the Quaternary to the lower Cretaceous time.

The study area contains three different aquifers in addition to a shale layer that lies between the second and third aquifers. The first aquifer is the shallow one and belongs to the Quaternary age and consists of coarse sand, gravel, silt, some intercalations of clay, and fine to medium sand. The second aquifer in the middle belongs to both the Miocene and Eocene ages and contains limestone, some intercalations of clay, sand, and gravel. Finally, the third aquifer is the deep one that belongs to the Cretaceous age and consists of sandstone with some intercalations of shale.

4. ANALYSES OF DATA

Visual MODFLOW software was used to develop the model for the study area using the gathered data, as illustrated in Figure (2). The bottom levels of boreholes in the study area were interpolated as well as interpolation of ground level values obtained from Aster GDEM v.2 worldwide elevation data (1 arc second resolution).

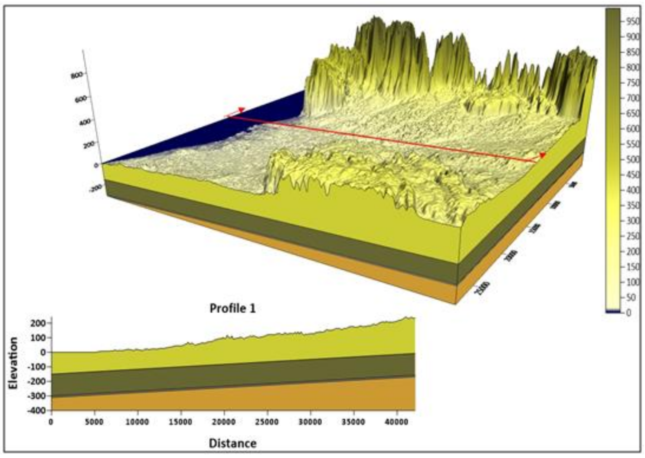

FIGURE (2). The Model of the Study Area.

The classification of boundary conditions and their equivalent mathematical representations were discussed by Anderson and Woessner, [13], and Reilly, [14]. Only three types of boundary conditions were represented in the study area, as shown in Figure (3). The Gulf of Suez in the eastern direction was assigned as a constant head boundary, while the northwest-southwest and western directions on the opposite side were assigned as no-flow boundary. At the outlet of the wadis in the study area, a specified flow boundary was assigned.

The model domain was divided into 46 zones of initial hydraulic conductivity values for the three aquifers where the values ranged between 1.35 m/d to 15.20 m/d. The average values were assigned to each zone and these values depended on previous studies in the study area, WRRI, [15], and El Osta et al., [16].

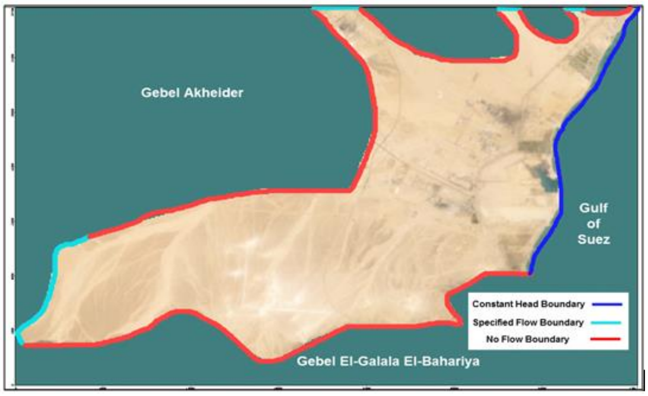

FIGURE (3). Hydraulic Boundaries of the Study Area.

There are two main resources of groundwater recharge in the study area: the rainfall and the floods in the wadis. The initial recharge values from these sources were estimated using two methods. These methods are the Soil Conservation Service curve number (SCS) method, NRCS, [17], and Cronshey, [18], and the Water Balance method, Gomaa et al., [19]. The initial recharge rate from rainfall was 1.10 x10^{-5} m/day and the flow rate values from the floods of wadis were 21.23, 32.82, 92.00, and 416.55 m^3/day for wadis Hommath, Hagoul, Bada, and Ghweiba, respectively, EL-HAZEK et al., [12].

The model was calibrated and validated for two phases: (1) steady-state condition using MODFLOW and PEST numeric engines and (2) dynamic state condition using SEAWAT numeric engine.

In the first phase, the steady state calibration was done using an automated parameter estimation code (PEST) as well as MODFLOW, where the initial values of hydraulic conductivity were adjusted to have calculated values close to the observed ones. The model was calibrated with 9 observed head values measured in 2013 and validation was done using additional 7 observed head values in the same year. The calibrated values of hydraulic conductivity for the three aquifers ranged between 0.17 m/d to 25 m/d.

The second phase included the dynamic state calibration using the SEAWAT numeric engine. This variable density numerical model was run for 400 years to reach the equilibrium condition between freshwater and seawater in the mixing zone. The model was calibrated with 7 observed head values measured in 2013 and validation was done using additional 6 observed head values in the same year.

5. RESULTS AND DISCUSSIONS

5.1 Groundwater Head

The calibrated values of hydraulic conductivity for the three aquifers ranged between 0.17 m/d to 25 m/d. The calibration results showed a good agreement between the calculated (X_{cal}) and observed (X_{obs}) heads where the maximum and minimum difference between them obtained a Root Mean Square (RMS) of 0.187 m. The normalized RMS was 3.66%, and the correlation factor between the calculated and observed groundwater levels was 0.995, as shown in Figure (4).

Three contour head maps for the three aquifers in the steady state were obtained, as represented in Figures (5), (6), and (7).

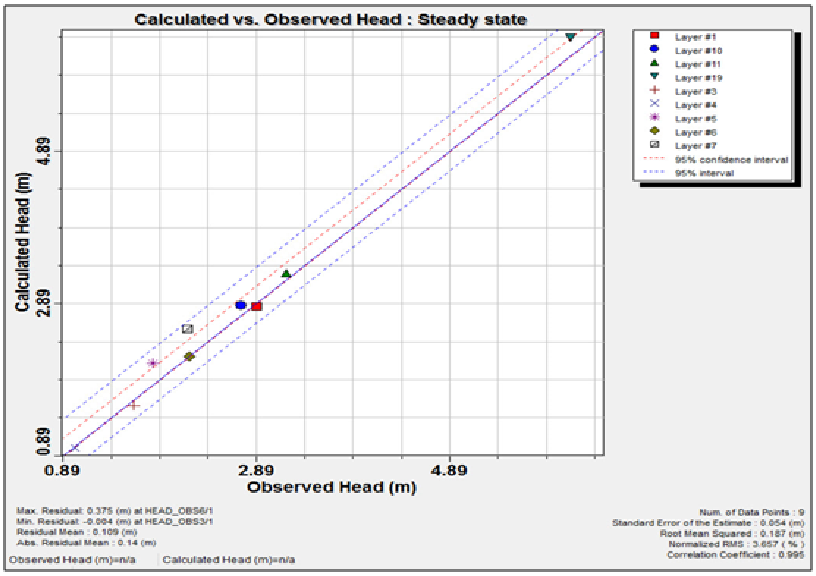

FIGURE (4). Calculated vs. Observed Groundwater Head for the Calibration Process.

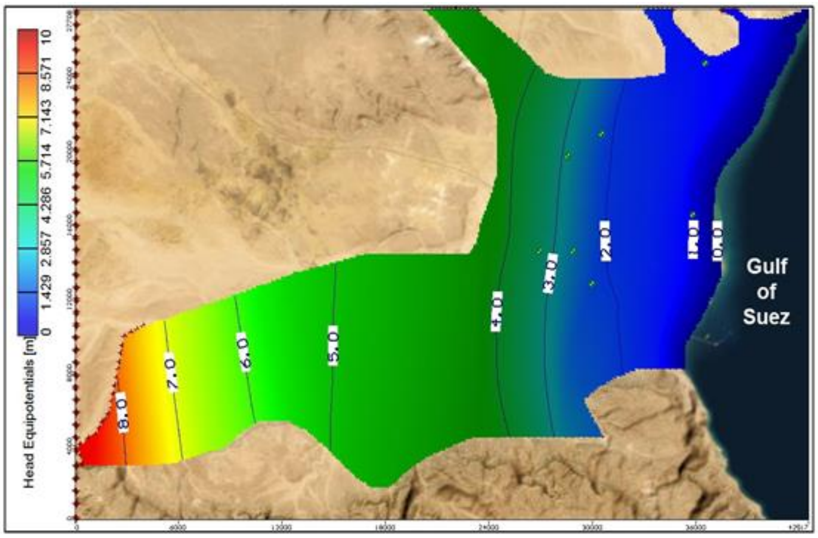

FIGURE (5). Calculated Groundwater Head for the Shallow Aquifer.

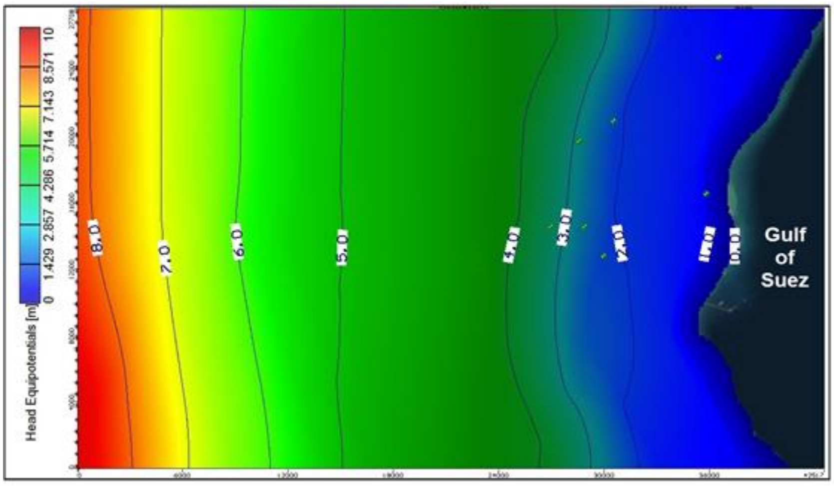

FIGURE (6). Calculated Groundwater Head for the Medium Aquifer.

After the calibration process, a validation process was done in the steady state to ensure the accuracy of the calibrated model. The results confirmed a good agreement between the calculated and observed heads where the maximum and minimum difference between them obtained an RMS of 0.24 m. The normalized RMS was 12.8%, and the correlation factor between the calculated and observed groundwater levels was 0.97, as shown in Figure (8).

5.2 Groundwater Salinity

The calibration in the dynamic state depends mainly on dispersivity which is one of the most affecting parameters on forming the mixing zone in the model. Dispersivity was calibrated manually until the equilibrium was reached between freshwater and saltwater where the values equaled 200 m, 20 m, and 2 m for longitudinal dispersivity, transverse dispersivity, and vertical dispersivity, respectively. Another affecting parameter is the molecular diffusion coefficient, which was taken as $1x10^{-9}$ m^2/s, Hussain and Javadi, [20]. The calibration results showed a good agreement between the calculated and observed values where the maximum and minimum difference between them obtained an RMS of 799 mg/L. The normalized RMS was 10.83%, and the correlation factor between the calculated and observed groundwater salinity values was 0.95, as shown in Figure (9).

Three contour salinity maps for the three aquifers in the dynamic state are represented in Figures (10), (11), and (12).

A vertical cross-section showed the mixing zone of the study area where the salinity contour line 10000 mg/L intruded up to distances of 1.06 km for the shallow aquifer and 2.26 km for both the middle and deep aquifers measured from the coastline in landward. It was concluded that the medium and deep aquifers were affected by seawater intrusion more than the shallow one. It was also found that the shale layer which existed between the medium and deep aquifers obstructed seawater intrusion slightly explaining the curved contour lines of salinity towards the sea at depths from 250 m to 350 m, as shown in Figure (13).

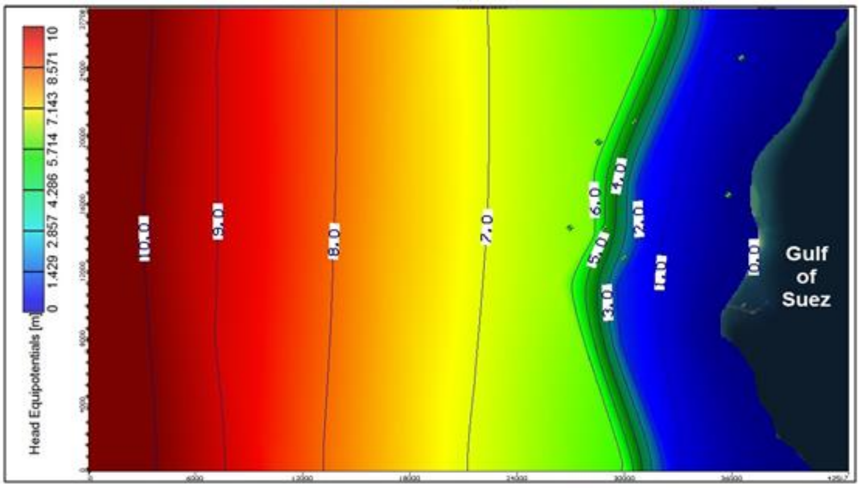

FIGURE (7). Calculated Groundwater Head for the Deep Aquifer.

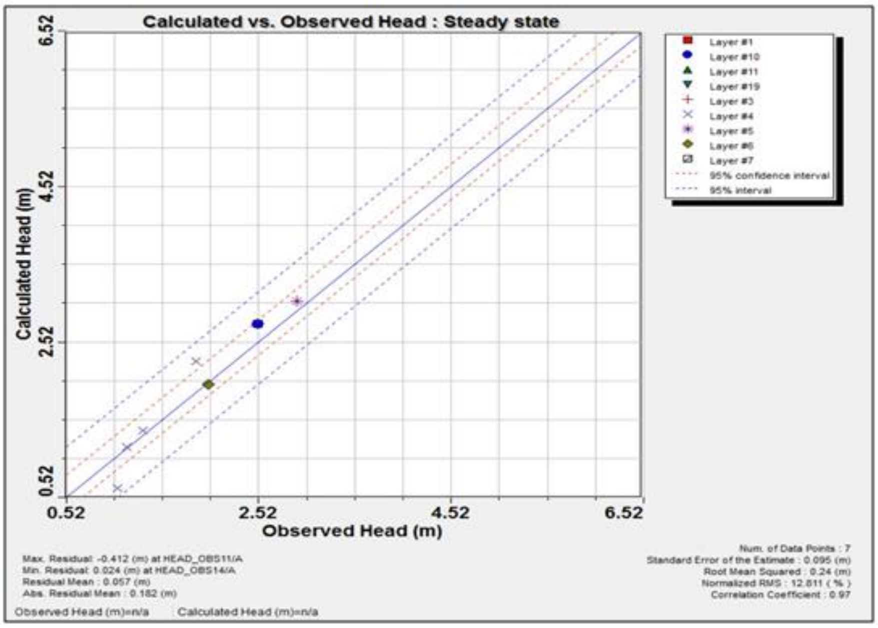

FIGURE (8). Calculated vs. Observed Groundwater Head for the Validation Process.

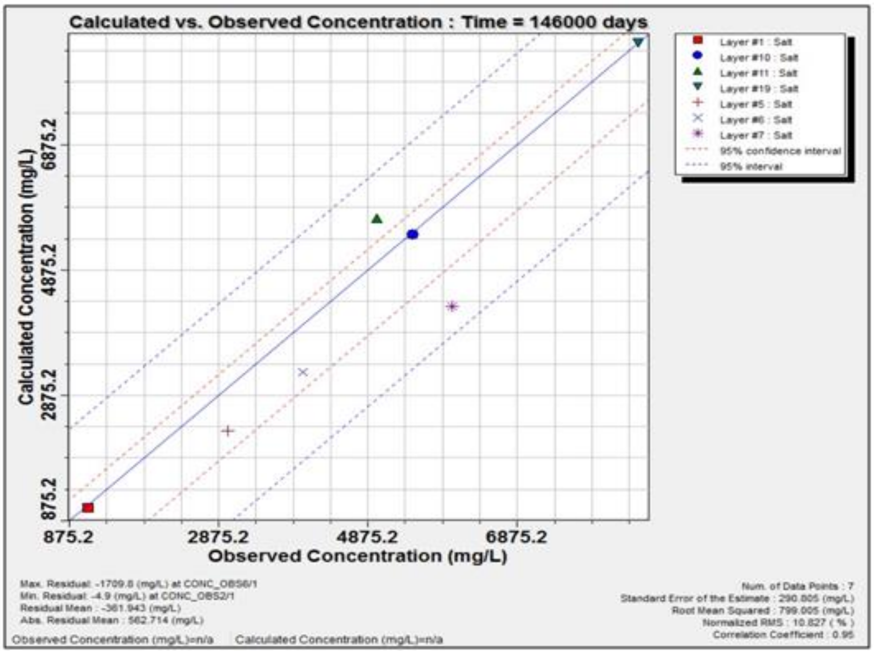

FIGURE (9). Calculated vs. Observed Groundwater Salinity for the Calibration Process.

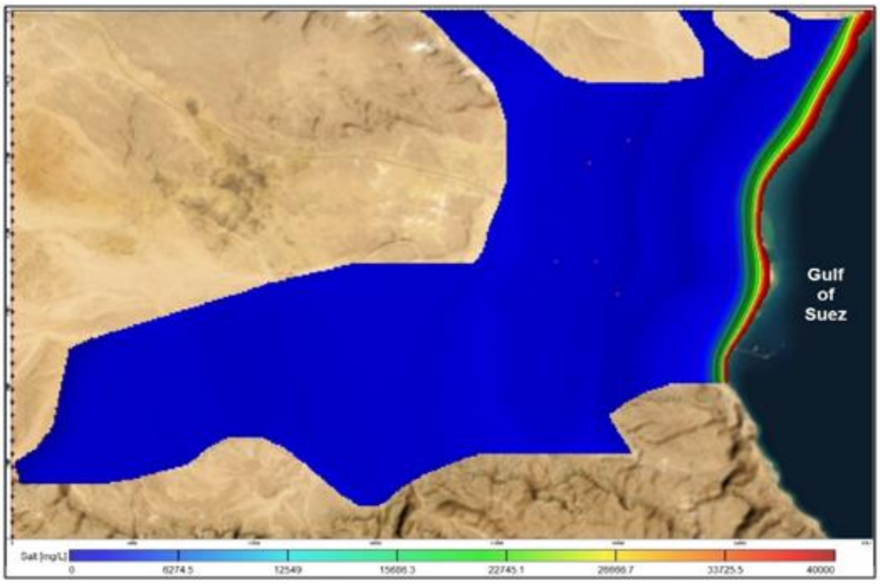

FIGURE (10). Calculated Groundwater Salinity for the Shallow Aquifer.

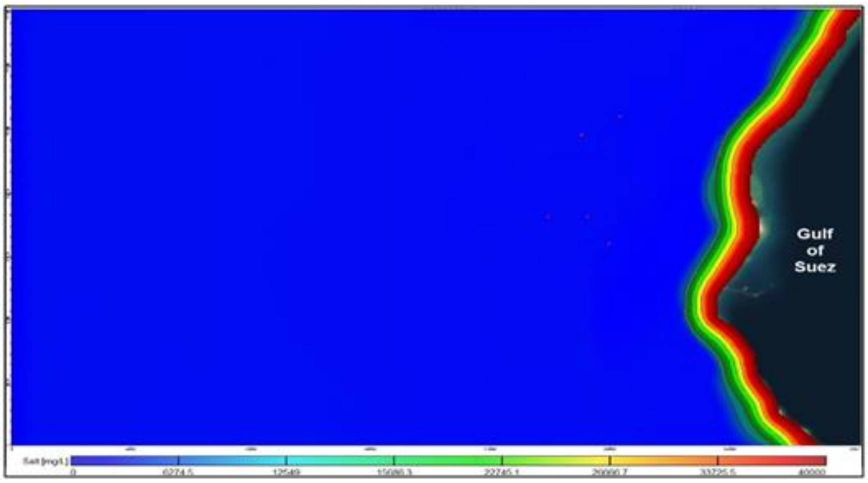

FIGURE (11). Calculated Groundwater Salinity for the Medium Aquifer.

After the calibration process, a validation process was done in the dynamic state to ensure the accuracy of the calibrated model. The results confirmed a good agreement between the calculated and observed values of salinity where the maximum and minimum difference between them obtained an RMS of 1131.5 mg/L. The normalized RMS was 14.14%, and the correlation factor between the calculated and observed salinity values was 0.946, as shown in Figure (14).

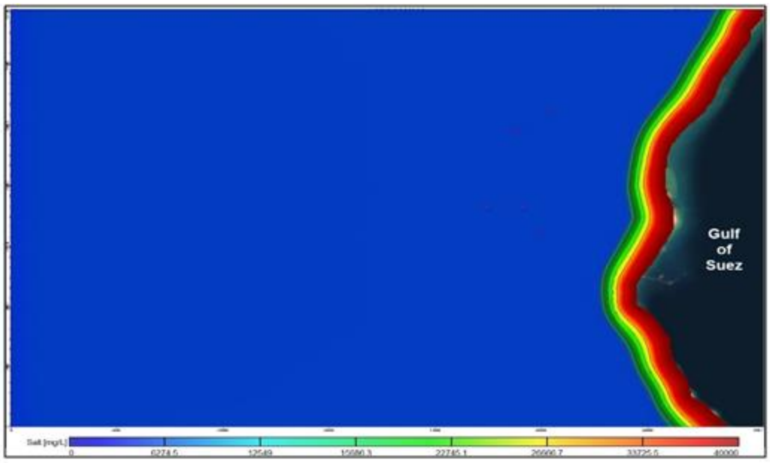

FIGURE (12). Calculated Groundwater Salinity for the Deep Aquifer.

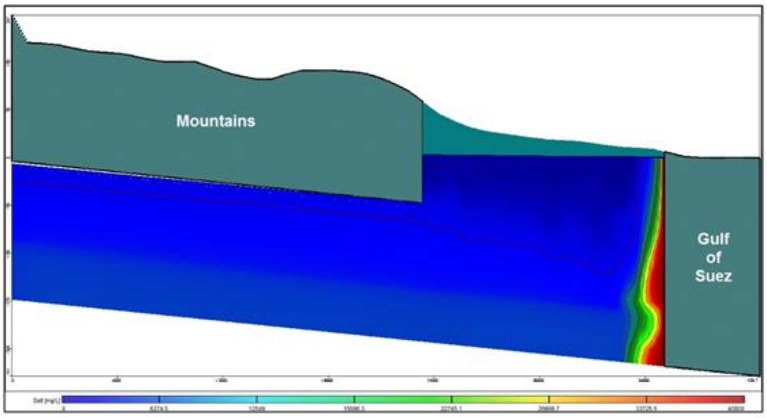

FIGURE (13). Cross-section of the Mixing Zone of the Study Area.

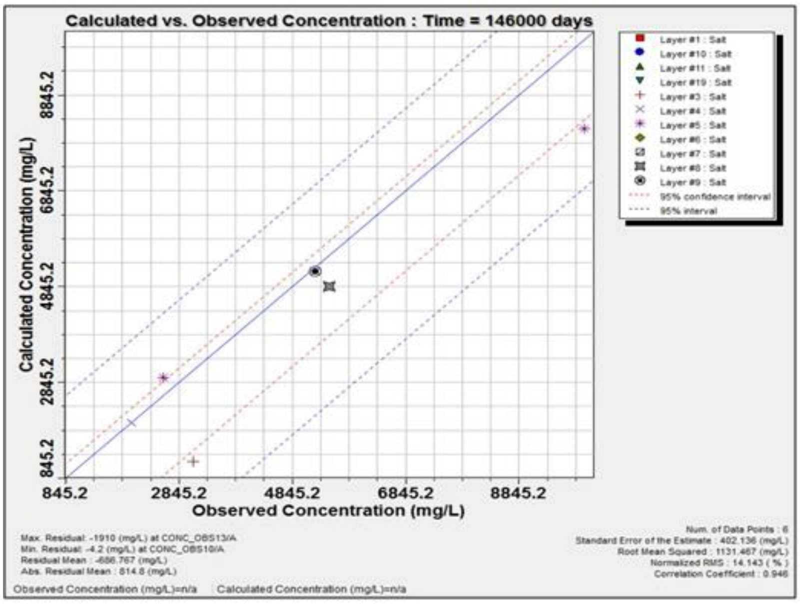

FIGURE (14). Calculated vs. Observed Groundwater Salinity for the Validation Process.

6. CONCLUSIONS

The main objective of this study was the investigation of the initial condition of seawater intrusion in the Ain Sukhna area, Egypt. Visual MODFLOW software was used to develop a model. Calibrating and validating the developed model for both the steady state and dynamic state were performed employing the numeric engines included in Visual MODFLOW software: PEST, MODFLOW, and SEAWAT.

The calibration and validation processes were done for both groundwater head and salinity observed values measured in 2013. The results showed a good fit between the observed and calculated values, giving a simulation for the initial condition of the seawater intrusion in the study area. Also, it was concluded that both the medium and deep aquifers were affected by the migration of seawater inland more than the shallow aquifer except for the zone where the shale layer was located, which obstructed seawater intrusion slightly.

ACKNOWLEDGMENTS

All thanks and appreciation to the staff of the Water Resources Research Institute who contributed to the completion of this work.

References

[1] Abd-Elaty, I., Zelenakova, M., Krajnikova, K., and Abd-Elhamid, H. F. (2021). “Analytical Solution of Saltwater Intrusion in Coastal Aquifers Considering Climate Changes and Different Boundary Conditions”. Water. 13. 995. 10.3390/w13070995.

[2] Armanuos, A. M., Ibrahim, M. G. E., Negm, A., Takemura, J., Yoshimura, C. and Mahmod, W. E. (2022). “Investigation of Seawater Intrusion in the Nile Delta Aquifer, Egypt”. Journal of Engineering Research. 10.21608/erjeng.2022.113766.1046.

[3] El Shinawi, A., Kuriqi, A., Zelenakova, M., Vranayova, Z., and Abd-Elaty, I. (2022). “Land subsidence and environmental threats in coastal aquifers under sea level rise and over-pumping stress”. Journal of Hydrology. 608. 127607. 10.1016/j.jhydrol.2022.127607.

[4] Yang, J., Graf, T., and Ptak, T. (2019). “Combined influence of weir construction and sea-level rise on freshwater resources of a coastal aquifer in northern Germany”. Hydrogeology Journal. 27. 1-11. 10.1007/s10040-019-02009-9.

[5] Janardhana, M. R. and Khairy, H. (2019). “Simulation of seawater intrusion in coastal aquifers: a case study on the Amol–Ghaemshahr coastal aquifer system, Northern Iran”. Environmental Earth Sciences. 78. 10.1007/s12665-019-8711-4.

[6] Ranjbar, A., Cherubini, C., and Saber, A. (2020). “Investigation of transient sea level rise impacts on water quality of unconfined shallow coastal aquifers”. International Journal of Environmental Science and Technology. 17. 10.1007/s13762-020-02684-2.

[7] Mastrocicco, M., Busico, G., Colombani, N., Vigliotti, M., and Ruberti, D. (2019). “Modelling Actual and Future Seawater Intrusion in the Variconi Coastal Wetland (Italy) Due to Climate and Landscape Changes”. Water. 11. 15. 10.3390/w11071502.

[8] Brkić, M. and Srzić, V. (2021). “Modeling of seawater intrusion into coastal aquifers in laboratory conditions”. E-Zbornik, elektronički zbornik radova Građevinskog fakulteta. 11. 29-41. 10.47960/2232-9080.2021.21.11.29

[9] Na, J., Chi, B., Zhang, Y., Li, J., and Jiang, X. (2019). “Study on the influence of seawater density variation on sea water intrusion in confined coastal aquifers”. Environmental Earth Sciences 78, 669 (2019). https://doi.org/10.1007/s12665-019-8684-3

[10] Guo, W. and Langevin, C. D. (2002). “User’s Guide to SEAWAT: A Computer Program for Simulation of Three-Dimensional Variable-Density Groundwater Flow”.

[11] Zheng, C. and Wang, P. P. (1999). “MT3DMS: A modular threedimensional multi-species transport model for simulation of advection, dispersion, and chemical reactions of contaminants in groundwater systems”. Documentation and User’s Guide, Contract Report SERDP-99-1. Vicksburg, Miss.: U.S. Army Engineer Research and Development Center. Available at: http://hydro.geo.ua.edu/mt3d/.

[12] El-Hazek, A. N., AbdelMageed, N. B., Mekhemer, H. M., and Amin, D. H. (2020). “Groundwater Evaluation and Management in Ain Sukhna, Egypt”. Asian Journal of Engineering and Technology. 8. 44-54. 10.24203/ajet.v8i1.6063.

[13] Anderson M. and Woessner W. (1992). “Applied groundwater modeling. Simulation of Flow and Advective Transport”.San Diego, California: Academic Press Inc.

[14] Reilly T. (2001). “System and Boundary conceptualization in ground-water flow simulation. Techniques of water resources investigations of the U.S. Geological Survey”. Book 3, Applications of Hydraulics. Chapter B8. Department of Interior. U.S. Geological Survey.

[15] Water Resources Research Institute (WRRI) (2013). “Technical Reports of Upper, Middle and Lower Wells in Wadi Bada – Ain Sukhna – Egypt”. Internal Report.

[16] El Osta M. M., El Sheikh A. El., and Barseem M. S. (2010). “Comparative Hydrological and Geoelectrical Study on the Quaternary Aquifer in the Deltas of Wadi Badaa and Ghweiba, El Ain El Sukhna Area, Northwest Suez Gulf, Egypt”. International Journal of Geophysics, Volume 2010, Article ID 585243, 15 pages.

[17] NRCS (2009) b. Part 630, Hydrology National Engineering Handbook, Chapter 7: Hydrologic Soil Groups.

[18] Cronshey R. (1986). “Urban Hydrology for Small Watersheds”. US Department of Agriculture, Soil Conservation Service, Engineering Division.

[19] Gomaa M. A., Mohallel S. A., and Elsheikh A. E. (2016). “Estimation of Recharge Quantity of the Fractured Basement Aquifer in the Southern Portion of Eastern Desert, Egypt; Critical Importance of the Hydrological and Chemical Criteria”. Middle East Journal of Applied Sciences, 6, 759-773.

[20] Hussain, M. S. and Javadi, A. (2015). “The Impacts of Different Aquifer Parameters on Seawater Intrusion in Coastal Aquifers Subjected to Sea Level Rise”. Conference: Workshop on Advances in Numerical Modelling of Hydrodynamics, HYdro2015, Sheffield University, 24-25 March 2015, At Sheffield, UK.